19th Australasian Fluid Mechanics Conference
Melbourne, Australia
8-11 December 2014

Numerical modelling of turbulent flow around an inclined ellipsoid

A. Phua[1], T.J. Barber[1], T. Rogers[2] and G.C. Doig[1,3]

[1]School of Mechanical and Manufacturing Engineering
UNSW Australia, New South Wales 2052, Australia

[2] School of Biological, Earth and Environmental Sciences
UNSW Australia, New South Wales 2052, Australia

[3]Aerospace Engineering Department
California Polytechnic State University, California 93407, United States of America

Abstract

This paper documents the assessment of the k-ω shear stress transport (SST) and large eddy simulation (LES) turbulence modelling approaches in the prediction of separated flow. A case of a 4.2:2:1 ellipsoid inclined at an angle of –10.2° was used to generate adverse flow conditions.

Numerical simulations were completed for Reynolds numbers (Re) 0.6×10^6, 2.5×10^6, 3.0×10^6 and 4.0×10^6, utilising water as the working fluid. Pressure and force predictions showed agreement within 5% of experimental values between Reynolds numbers of $2.5\text{-}4.0 \times 10^6$ for SST. However, the SST model did not cope well with lower velocity flows, predicting an 87% increase in drag for $Re = 0.6 \times 10^6$. A single run was completed utilising the LES model at $Re = 4.0 \times 10^6$ and predicted drag within 1% of experimental values. Wake flow was also correctly simulated, with LES able to present much finer transient detail. This study has relevance to the simulation of marine mammals.

Introduction

This study aimed to evaluate numerical modelling methods for simulating flow about marine mammals. Relevant numerical studies on 6:1 spheroids have produced accurate results for Reynolds-Averaged Navier-Stokes (RANS) [3], detached eddy simulation (DES) [6] and large eddy simulation (LES) [5] turbulence models, proving their capabilities to handle the turbulent flow. With a fineness ratio (FR = length : max width) of 6 and axisymmetric form, 6:1 spheroids may be too slender and simple for assessing numerical simulation methods for marine mammals.

The ellipsoid is an easily defined shape which presents similar form characteristics to a marine mammal. Clarke [2] completed a comprehensive investigation of the flow around a 4.2:2:1 ellipsoid, equating to a FR of 2.1. Along with a non-axisymmetric form, this ellipsoid is a more suitable geometry for assessing numerical methods for simulating marine mammals.

Clarke [2] obtained experimental results in a cavitation tunnel at Reynolds numbers between 0.6×10^6 and 4.0×10^6 utilising angles of attack from –0.2° to –10.2°. Collected data included body forces and moments, pressure distributions, surface flow and boundary layer survey. A limited numerical simulation of the experiments was also conducted by Clarke using the k-ε realizable turbulence model, which results showed reasonable accuracy compared to experimental values.

This study will model a lower fineness ratio ellipsoid utilising the k-ω shear stress transport (SST) and LES turbulence models which were effective on the spheroid geometry and assess the impact of this change in geometry. It will also determine the detail to which SST and LES can predict flow about an ellipsoid and if LES is necessary to capture relevant flows.

Numerical Simulation

To assess the capabilities of k-ω SST and LES turbulence approaches, the case of an ellipsoid inclined at –10.2° to the flow was selected. The simulation setup was based on the cavitation tunnel experiments by Clarke [2], using a 330 mm long 4.2:2:1 ellipsoid with fresh water ($\rho = 998.2$ kg/m^3) as the working fluid. The ellipsoid and mounting peripherals caused a blockage of 7.8% and would have an effect on the results [4]. To reproduce this, the supporting foil and sting utilised in the experiment and cavitation tunnel working section were included into the simulation geometry. The ellipsoid centre is used as the coordinate datum with X as the transverse axis, Y as the longitudinal axis and Z as the vertical axis relative to the ellipsoid. The azimuth angle was measured from the 12 o'clock position, positive clockwise when observing from the front (Figure 1: note that axis has been offset along Z-axis for clarity).

The simulations were assumed to be incompressible and single phase. As free stream velocity was constant and there was no dynamic movement in the model, it was assumed for SST based simulations were a steady case. All surfaces, including cavitation tunnel walls, were assumed to be perfectly smooth. As there was no boundary layer survey completed on the cavitation tunnel walls, the inlet profile was mapped from an outlet flow profile of the empty cavitation tunnel to approximate.

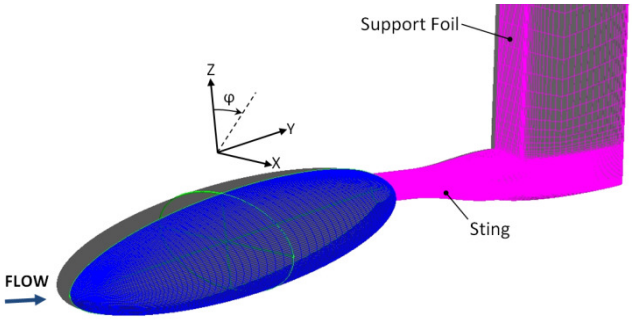

Figure 1: Schematic setup of ellipsoid and mounting peripherals with surface mesh (half) applied.

The k-ω SST turbulence model was selected for use as it has shown good performance in handling separated flows [1]. SST simulations utilised a symmetry plane along the longitudinal vertical plane (Figure 1). Steady SST simulations were completed at Reynolds numbers of 0.6×10^6, 2.5×10^6, 3.0×10^6 and 4.0×10^6 based on length, equating to 1.82, 7.56, 9.08 and 12.1 ms^{-1} respectively. A mesh size of 4,174,976 was chosen for the symmetrical SST simulations following a mesh refinement study conducted at Re = 4.0×10^6 (Table 1).

Table 1: Mesh refinement study. SST, Re = 4.0×10^6

Elements	C_D	Difference
1051284	0.0816	NA
2387410	0.0800	2.0%
3297990	0.0786	1.8%
4174976	0.0781	0.6%

For an initial comparison, a transient run was completed utilising LES at a Reynolds number of 4.0×10^6. Due to the unsteady nature of the LES turbulence model, a full domain mesh of 21,289,226 was created by refining and reflecting the grid utilised in the SST simulations about the symmetry plane after trial runs utilising the mirrored SST grid without any refinements (8,349.952 elements), yielded an 8.7% underestimation of experimental drag values. The grid convergence index (GCI) between the fine and coarse LES meshes was 0.04.

The Wall-Adapting Local Eddy-Viscosity (WALE) subgrid scale model was selected for use with the LES based simulations as it was designed to handle transitional flow [1]. WALE models eddy viscosity according to:

$$\mu_t = \rho L_S^2 \frac{\left(S_{ij}^d S_{ij}^d\right)^{3/2}}{\left(\bar{S}_{ij}\bar{S}_{ij}\right)^{5/2} + \left(S_{ij}^d S_{ij}^d\right)^{5/4}} \quad (1)$$

Where:

$$L_S = min\left(\kappa d\,, C_W V^{1/3}\right) \quad (2)$$

$$S_{ij}^d = \frac{1}{2}\left(\bar{g}_{ij}^2 + \bar{g}_{ij}^2\right) - \frac{1}{3}\delta_{ij}\bar{g}_{kk}^2\,;\ \bar{g}_{ij} = \frac{\partial \overline{u_i}}{\partial x_j} \quad (3)$$

The WALE model constant C_W was set at a value of 0.325 as it was found to produce satisfactory results for a wide range of flows [1]. Another transient simulation using SST was also completed at Re = 4.0×10^6 for comparison.

Results and Discussion

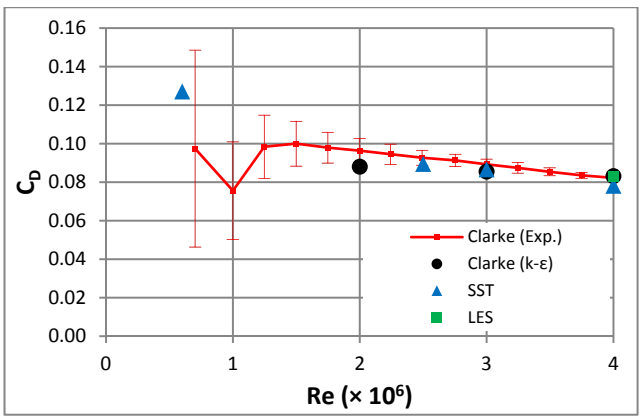

Figure 2: C_D values versus Reynolds number

The drag predictions (Figure 2) from the SST had very good agreement with experimental measurement (within 5%) for Reynolds 2.5-4.0 × 10^6. The SST model also responded well to changes in flow velocity, mimicking the decreasing C_D with increasing Reynolds number. In comparison, the k-ε realizable C_D by Clarke [2] did not react strongly with changes in Reynolds number. Arguably, the SST model was the more reliable of the RANS models for this simulation despite the fact that at Re = 4.0×10^6, the SST model underestimated C_D by 4.9% while the realizable k-ε over predicted it by only 1.2%. The simulation utilising LES at Reynolds 4.0×10^6 predicted a C_D only 1.4% less than experimental.

The SST model does not seem to handle lower Re flows as well, with much greater deviation from experimental values. However, this was still within the range of experimental error, which was up to 87% at lower Reynolds numbers. Due to the large variance of the low Reynolds results, analysis has focused on the higher range of free stream velocities.

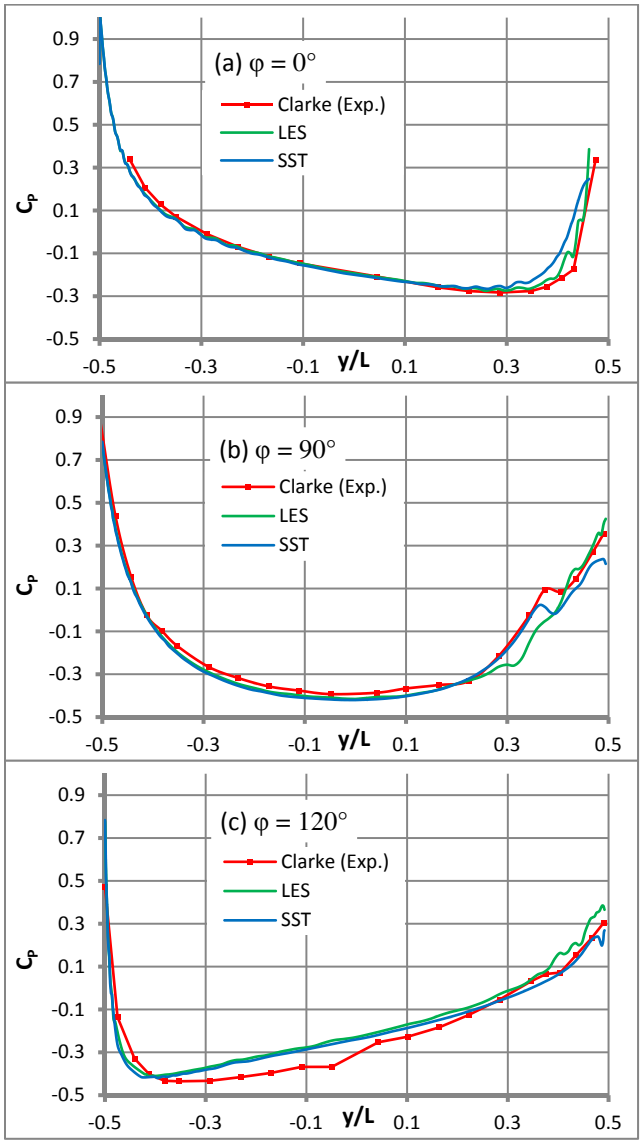

Figure 3: C_p versus y/L at Re = 4.0×10^6

Pressure distribution was calculated at azimuth angles mapped to the ellipsoid surface according to the following equation:

$$\varphi_e = \tan^{-1}\left(\frac{Z}{X}\tan\varphi\right) \quad (4)$$

Where:

$$Z = height\ of\ ellispod\ (mm)$$
$$X = width\ of\ ellipsoid\ (mm)$$
$$\varphi = azithumal\ angle\ (°)$$

Pressure along each azimuth angle was non-dimensionalised for direct comparison to results by Clarke. Figure 3 shows plots of calculated C_p and experimental results at azimuth angles of 0°, 90° and 120°. The C_p values for the LES prediction have been averaged from 0.05, 0.55 and 1.05 second time steps.

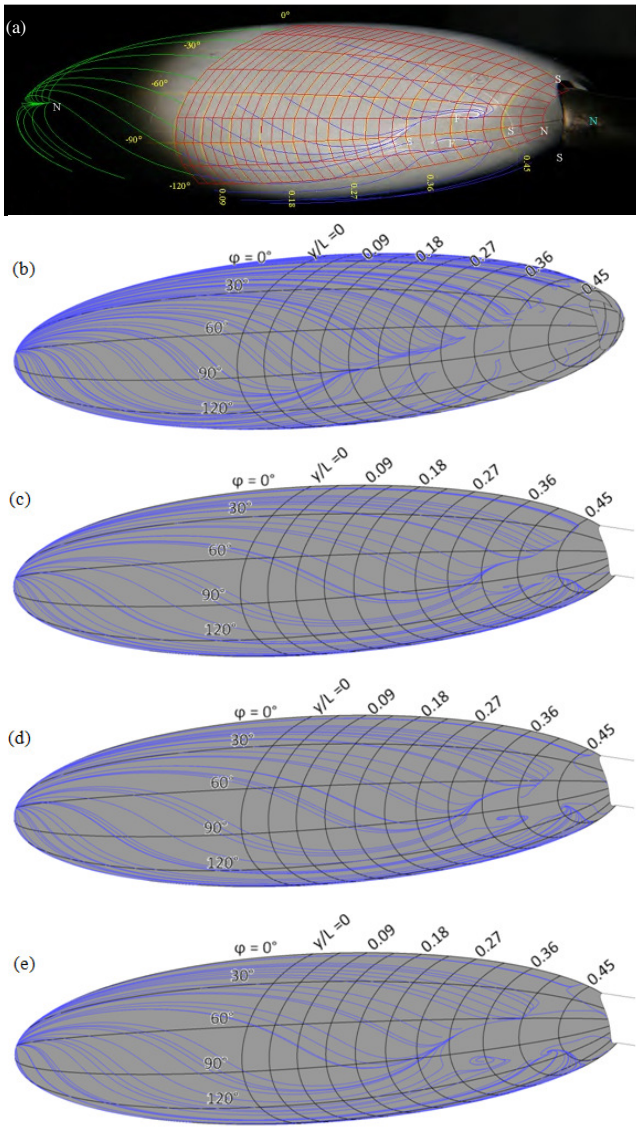

Figure 4: Surface flow visualisations. (a) Experimental by Clarke, Re = 4.0 ×10⁶ (b) LES @ 0.55 s, Re = 4.0 × 10⁶ (c) SST, Re = 4.0 × 10⁶ (d) SST, Re = 2.5 × 10⁶ (e) SST, 0.6 × 10⁶

Along the 0° and 90° azimuth angles, simulations utilising SST and LES turbulence models predicted C_p values with good correlation to experimental data at the front of the ellipsoid. Towards the rear however both turbulence models had a tendency to predict a separation point further upstream than experimental. It was also observed that LES out performs SST at the 0° azimuth angle while the converse is true at φ = 90°. This result reflects those from 6:1 spheroid cases; Wikstrom [5] where LES C_p predictions were more accurate at φ = 0° opposed to other angles and Xiao [6] where SST was its most accurate when estimating C_p at φ = 90°.

At φ = 120°, experimental measurements showed separation occurring at y/L ≈ 0. This was not predicted by the numerical simulations. There was a notable difference in C_p at this point which progressed along the azimuth. As the numerical predictions for $-0.5 < y/L < 0.3$ along the 120° azimuth were nearly identical.

Surface flow patterns generated by the SST simulations (Figure 4c-e) were able to define areas of flow separation towards the rear of the ellipsoid starting around y/L = 0.35 and propagating radially to φ = 0° and 180° by y/L = 0.45 in the case of $Re = 4.0 \times 10^6$. Separation at other Reynolds numbers were similar, with the progression of the separation region towards the front of the ellipsoid with decreasing Re was reflective of the reduced momentum and matched experimental observations. Foci in the rear separated zones were predicted by the SST turbulence model. On the other hand, foci were not to be expected from snapshots generated from the LES solution.

The LES model (Figure 4b) was able to capture the convergent streamline beginning at y/L ≈ 0.14 and φ ≈ 105°, which is indicative of open separation. The open separation on the mid-flank was seen in progress forward with decreasing Reynolds (Figure 4); the SST simulations were unable to detect this at any Reynolds number.

The SST simulations predicted a primary vortex structure shedding from the ellipsoid along the convergent streamline and sucked towards the lower side and detaching from the ellipsoid in the rear separation region (Figure 5). The rotational intensity and size of the primary vortex increased, while only the rotational intensity of the secondary vortex increased with increasing Reynolds number.

The flow patterns predicted by the LES simulation showed multiple smaller counter-rotating vortices forming around the primary and secondary vortex structures as the vortex grows and dissipates. The vortices can be seen developing in size from the 0° azimuth angle to a maximum about the limiting stream line, shedding off and creating the primary wake vortex.

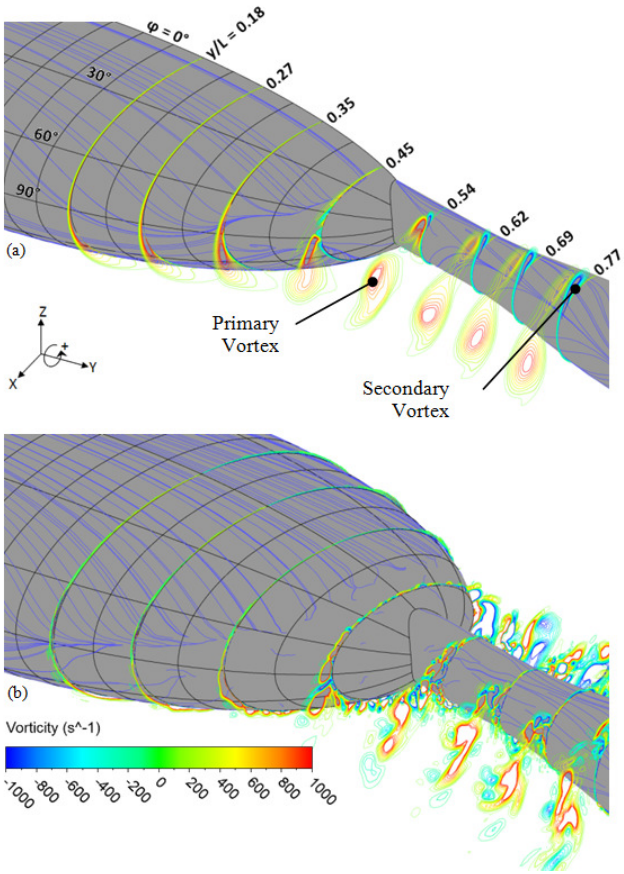

Figure 5: Stream wise vorticity at Re = 4.0 × 10^6. (a) SST. (b) LES

There was also evidence of a convergent streamline along the sting from which a secondary vortex propagated. The secondary vortex rotated in the opposite direction to the primary vortex. At higher Reynolds numbers, the primary vortex was drawn to the secondary and at 4.0×10^6 shows characteristics of destructive interference.

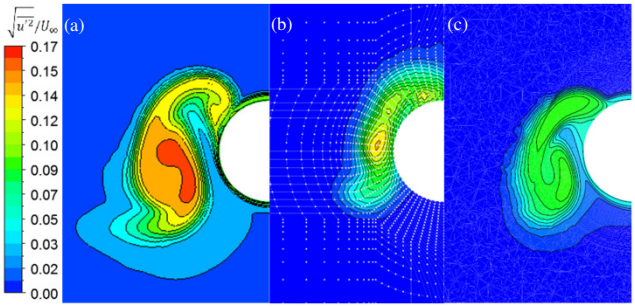

Figure 6: Velocity fluctuations at y/L = 0.77, Re = 3.0 × 10^6. (a) SST (b) Clarke (Exp.) (c) Clarke (k-ε)

As seen in Figure 6, vortex structures were inferred from velocity fluctuations, measured experimentally and calculated from kinetic energy (k) from numerical results. The SST turbulence model showed improvement in predicting wake flow compared to the realizable k-ε turbulence based numerical simulations by Clarke. The SST model predicted larger fluctuating velocity components with similar magnitude to what was measured. However, the both SST and realizable k-ε models predicted the location of the primary vortex core twice as far away from the sting than measured and reduced kinetic energy dissipation as seen by larger regions of velocity fluctuations.

Conclusions

A 4.2:2:1 ellipsoid has been modelled numerically at –10° angle of attack in water to assess the abilities of the SST and LES turbulence models in predicting separated flow around a broad body. Both SST and LES methods were able to provide stable results for high Reynolds number flows. Numerical predictions of pressure, body forces and moments were reasonably accurate in comparison to experimental results. SST showed improved accuracy over previous force and wake predictions utilising the realizable k-ε turbulence model. In addition, due to the inherent nature of averaged turbulence models, the SST approach was not able to capture the intricacies of the growth and dissipation of vortices which the LES method was able to.

SST and LES turbulence models are both capable of handling separated flow at high Re over a low fineness ratio body. The methods implemented in this study should function well for the numerical analysis of marine mammals. Increasing attack angle range and introducing dynamic motions into simulation are future avenues of investigation to develop a better understanding of low fineness ratio bodies and their hydrodynamic performance.

References

[1] ANSYS Inc., *ANSYS FLUENT Theory Guide* Canonsburg, ANSYS Inc, 2012

[2] Clarke, D.B., *Experimental and Computational Investigation of Flow about Low Aspect Ratio Ellipsoids at Transcritical Reynolds Numbers,* Ph.D. thesis, University of Tasmania, 2009

[3] Kim, S., Rhee S.H., Cokljat, D., Application of Modern Turbulence Models to Vortical Flow Around a 6:1 Prolate Spheroid at Incidence, *41st Aerospace Sciences Meeting and Exhibit,* AIAA, 2003

[4] Pope, A., *Wind tunnel Testing* New York, John Wiley & Sons, 1954

[5] Wikstrom, N., Svennberg, U., Alin, N., Fureby, C., Large Eddy Simulation of the flow around an inclines prolate spheroid, *Journal of Turbulence,* **5**, 2004, 37-41

[6] Xiao, Z.X., Zhang, Y.F., Huang, J.B., Chen H.X., Fu, S., Prediction of separation flows around a 6:1 prolate spheroid using RANS/LES hybrid approaches, *Acta Mechanica Sinica*, **23**, 2007, 369-38